8-26-2010

# Structure of S30 with S32(p,t)S30 and the thermonuclear P29(p,γ)S30 reaction rate

K. Setoodehnia
*McMaster University*

A. A. Chen
*McMaster University*

J. Chen
*McMaster University*

J. A. Clark
*Yale University*

C. M. Deibel
*Yale University*

*See next page for additional authors*



## Recommended Citation

Setoodehnia, K., Chen, A., Chen, J., Clark, J., Deibel, C., Geraedts, S., Kahl, D., Parker, P., Seiler, D., & Wrede, C. (2010). Structure of S30 with S32(p,t)S30 and the thermonuclear P29(p,γ)S30 reaction rate. *Physical Review C - Nuclear Physics, 82* (2) https://doi.org/10.1103/PhysRevC.82.022801

PHYSICAL REVIEW C **82**, 022801(R) (2010)

# Structure of $^{30}$S with $^{32}$S$(p,t)^{30}$S and the thermonuclear $^{29}$P$(p,\gamma)^{30}$S reaction rate

K. Setoodehnia,[1,*] A. A. Chen,[1,2] J. Chen,[1] J. A. Clark,[3,4] C. M. Deibel,[3,4,5] S. D. Geraedts,[1] D. Kahl,[1,†] P. D. Parker,[3] D. Seiler,[6] and C. Wrede[3,7]

[1]*Department of Physics & Astronomy, McMaster University, Hamilton, ON L8S 4M1, Canada*
[2]*Excellence Cluster Universe, Technische Universität München, D-85748 Garching, Germany*
[3]*Wright Nuclear Structure Laboratory, Yale University, New Haven, Connecticut 06520, USA*
[4]*Physics Division, Argonne National Laboratory, Argonne, Illinois 60439, USA*
[5]*Joint Institute for Nuclear Astrophysics, Michigan State University, East Lansing, Michigan 48824, USA*
[6]*Physik Department E12, Technische Universität München, D-85748 Garching, Germany*
[7]*Department of Physics, University of Washington, Seattle, Washington 98195, USA*

(Received 2 July 2010; published 26 August 2010)

The structure of proton unbound $^{30}$S states is important for determining the $^{29}$P$(p,\gamma)^{30}$S reaction rate, which influences explosive hydrogen burning in classical novae and type I x-ray bursts. The reaction rate in this temperature regime had been previously predicted to be dominated by two low-lying, unobserved, $J^\pi = 3^+$ and $2^+$ resonances above the proton threshold in $^{30}$S. To search for these levels, the structure of $^{30}$S was studied using the $^{32}$S$(p,t)^{30}$S transfer reaction with a magnetic spectrograph. We have confirmed a previous detection of a state near 4700 keV, which had tentatively been assigned $J^\pi = 3^+$. We have also discovered a new state at 4814(3) keV, which is a strong candidate for the other important resonance ($J^\pi = 2^+$). The new $^{29}$P$(p,\gamma)^{30}$S reaction rate is up to 4–20 times larger than previously determined rates over the relevant temperature range. The uncertainty in the reaction rate due to uncertainties in the resonance energies has been significantly reduced.

DOI: 10.1103/PhysRevC.82.022801 PACS number(s): 26.30.Ca, 25.40.Hs, 27.30.+t, 97.10.Cv

Classical novae occur in binary systems through the ignition of unstable hydrogen burning in the envelope accreted from a main sequence star onto a white dwarf. Simulations show that peak temperatures reached in the thermonuclear runaway are typically in the 0.1–0.4 GK range [1]. The main nucleosynthesis paths in the runaway, and the abundances produced therein, can be connected to silicon isotopic abundance ratios ($^{29}$Si/$^{28}$Si and $^{30}$Si/$^{28}$Si) in presolar grains of potential nova origin [2–4]. To explore this connection, the thermonuclear reactions that most strongly affect the synthesis of silicon in novae must be determined and their rates understood. One such reaction is $^{29}$P$(p,\gamma)^{30}$S. In a study on the sensitivity of nova nucleosynthesis to uncertainties in thermonuclear reaction rates [5], a change in its rate by $10^4$, which was consistent with the rate limits from Ref. [6], resulted in significant changes in $^{29,30}$Si abundances by a factor of 3.

The $^{29}$P$(p,\gamma)^{30}$S reaction also influences type I x-ray bursts (peak $T \approx 1.5$ GK), which result from thermonuclear runaways in hydrogen- and helium-rich material accreted onto the neutron star surface in an x-ray binary system [7,8]. The energy generation and nucleosynthesis in the burst, along with its duration and light-curve structure, are very sensitive to the reaction flow through a few waiting-point nuclei along the $rp$- and $\alpha p$-process paths [9–11]. In particular, network calculations show that the waiting-point nucleus $^{30}$S ($t_{1/2} = 1.178$ s) is critical [9,12]: Its long half-life (comparable to typical burst rise times of a few seconds), along with the $(p,\gamma)$-$(\gamma,p)$ equilibrium established between $^{30}$S ($Q_{p\gamma} = 284(7)$ keV [13]) and $^{31}$Cl, results in a significant bottleneck for the reaction flow. In this context, $^{30}$S is produced by the $^{27}$Si$(p,\gamma)^{28}$P$(p,\gamma)^{29}$S$(\beta^+,\nu)^{29}$P$(p,\gamma)^{30}$S and $^{26}$Si$(\alpha,p)^{29}$P$(p,\gamma)^{30}$S sequences, depending on the phase and location of the explosive burning [9]. The $^{29}$P$(p,\gamma)^{30}$S reaction is the link leading to $^{30}$S production in both sequences and is one of the most important reactions in the overall flow as the burst temperature approaches its peak [14].

At these stellar temperatures (0.1–1.5 GK), the Gamow window of the $^{29}$P$(p,\gamma)^{30}$S reaction ($Q = 4399(3)$ keV [15]) spans $E_{\rm cm} \approx 100$–$1100$ keV. The reaction rate is thus dominated by contributions from isolated and narrow $^{29}$P + $p$ resonances corresponding to $^{30}$S states with $4.5 \lesssim E_x \lesssim 5.5$ MeV. The rate was evaluated by Wiescher and Görres [16] and more recently by Iliadis *et al.* [6]. The latter found that their calculated rate was dominated by two $3^+_1$ and $2^+_3$ proton unbound states in $^{30}$S, which had not yet been found experimentally. Their energies were predicted with the isobaric multiplet mass equation (IMME) to be 4733(40) keV and 4888(40) keV, respectively. This large uncertainty in the resonance energies $E_R$ translated, in turn, into a rate uncertainty of orders of magnitude [6], because the rate depends exponentially on $E_R$.

In a recent study of the $^{32}$S$(p,t)^{30}$S reaction, Bardayan *et al.* [17] discovered a state at 4704(5) keV that was proposed to be the predicted $3^+$ state. However, no experimental information on the energy of the other important level is presently available, and moreover, the structure of particle unbound states in $^{30}$S remains poorly understood [18]. Hence, further studies are strongly motivated, and experiments at several laboratories (e.g., NSCL [19], University of Notre Dame [20], University

*setoodk@mcmaster.ca
†Present address: Center for Nuclear Study (CNS), Graduate School of Science, University of Tokyo, Wako Branch at RIKEN, 2-1 Hirosawa, Wako, Saitama 351-0198, Japan.

 

TABLE I. Energies of $^{30}$S excited states (in keV) below 5.5 MeV measured in this work and previous studies. Spin and parity assignments are separated from the energies by a dash. States marked with "⋆" were used as energy calibration points in the present work (see text).

| Paddock [23] $^{32}$S$(p,t)^{30}$S | Caraça *et al.* [24] $^{28}$Si$(^3$He$,n\gamma)^{30}$S | Kuhlmann *et al.* [25] $^{28}$Si$(^3$He$,n\gamma)^{30}$S | Yokota *et al.* [26] $^{28}$Si$(^3$He$,n)^{30}$S$(p)$ | Fynbo *et al.* [27] $^{31}$Ar$(\beta^+)^{31}$Cl$(p)^{30}$S$(p)$ | Bardayan *et al.* [17] $^{32}$S$(p,t)^{30}$S | Present work $^{32}$S$(p,t)^{30}$S |
|---|---|---|---|---|---|---|
| g.s.–$0^+$ | | | | | g.s.–$0^+$ | |
| 2239(18)–$2^+$ | 2209.9(11) | 2210.7(5)–2 | | | 2210.7–$2^+$ | 2210.6⋆ |
| 3438(14)–$2^+$ | 3402.2(14) | 3402.6(5)–1,2 | | | 3402.6–$2^+$ | 3402.6⋆ |
| | 3664.2(13) | 3667.5(10) | | | | |
| 3707(25)–$(0^+)$ | | 3676(3)–1 | | | 3680(6)–$(1^+)$ | 3680(4) |
| | | | | | 4704(5)–$(3^+)$ | 4693(5) |
| | | | | | | 4814(3) |
| | | 5136(2)–$(4^+)$ | 5145(10) | | | 5136⋆ |
| | | | | | 5168(6)–$4^+ + 0^+$ | |
| 5207(22) | | | | 5217.4(7) | | 5226(3) |
| 5306(25) | | | 5288(10)–$3^-$ | | | 5318(4) |
| 5426(25) | | | 5425(10)–(1,2) | 5389(2) | 5383(8)–$(3^-,2^+)$ | 5396(4) |

of Tsukuba [21], and ANL [22]) are attempting to address these questions. Table I summarizes the work to date on the structure of $^{30}$S in the relevant energy range.

In the present work, the $^{32}$S$(p,t)^{30}$S reaction was studied with improved energy resolution relative to those of previous $(p,t)$ experiments [17,23], in order to confirm the existence of the proposed $3^+$ resonance from Ref. [17] and to search for the $2^+$ state that purportedly contributes strongly to the $^{29}$P$(p,\gamma)^{30}$S reaction rate.

The experiment was performed at the Wright Nuclear Structure Laboratory at Yale University. Protons were accelerated by the ESTU tandem Van de Graaff accelerator to 34.5 MeV with intensities of up to 90 enA and focused to a spot size of 2 mm in diameter on target. The target was 249 $\mu$g/cm$^2$ of CdS evaporated onto a 20 $\mu$g/cm$^2$ natural carbon foil. A free-standing 311 $\mu$g/cm$^2$ natural Si foil was used for calibration purposes. The target thickness uncertainty was determined to be about 10% from energy losses of $\alpha$ particles from an $^{241}$Am source. The reaction ejectiles were momentum-analyzed with an Enge split-pole magnetic spectrograph, with vertical and horizontal aperture settings of $\Delta\phi = \pm 40$ mrad and $\Delta\theta = \pm 20$ or $\pm 30$ mrad (the smaller $\Delta\theta$ setting was used at lower angles to avoid prohibitively high count rates in the spectrograph's focal plane detector). The tritons were focused at the spectrograph's focal plane ($\rho$ = 70–87 cm), and their momenta and energy losses ($\Delta E$) were measured with a position-sensitive ionization drift chamber [28]. Those that passed through this detector deposited their residual energy ($E$) in a plastic scintillator. The study was carried out over a 7-day period with a magnetic field strength of 10 kG for $\theta_{\rm lab} = 10^\circ$, $20^\circ$, $22^\circ$, and $62^\circ$.

The tritons were selected with software gates in histograms of $\Delta E$ and $E$ vs focal plane position (proportional to momentum), and spectra of their momenta were plotted for each spectrograph angle. Triton spectra at selected angles are shown in Fig. 1.

The background from $(p,t)$ reactions on the Cd and carbon in the CdS target was measured with a 200-$\mu$g/cm$^2$ Cd foil supported by a 20 $\mu$g/cm$^2$ substrate of natural carbon and with a 75 $\mu$g/cm$^2$ 95.6% isotopically enriched $^{13}$C foil. The main contaminant peak is from the $^{12}$C$(p,t)^{10}$C(g.s.) reaction, with its peak location away from the region of interest. Triton peaks corresponding to $^{30}$S states were clearly identified through kinematic analysis.

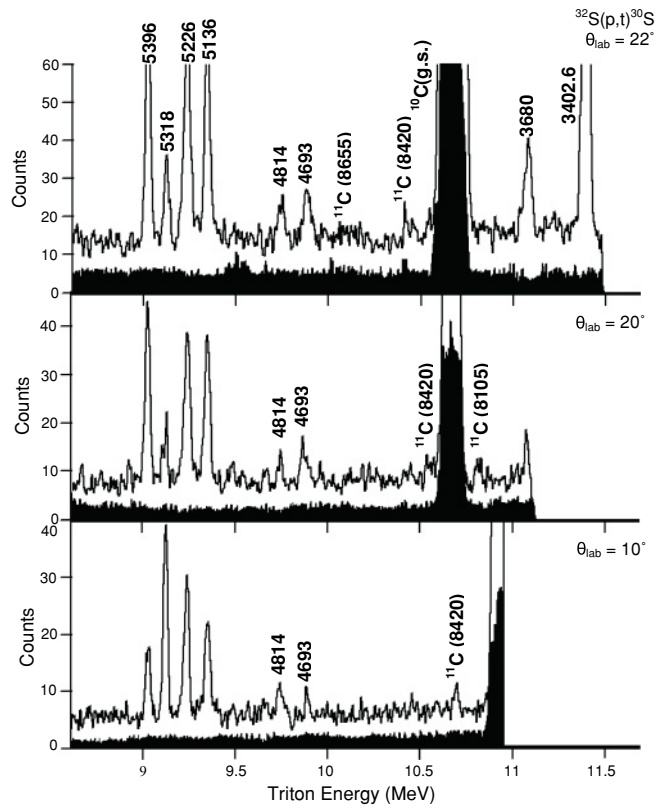


FIG. 1. Triton spectra from the $^{32}$S$(p,t)^{30}$S reaction. Peaks corresponding to $^{30}$S states are labeled with energies in keV. The solid histograms are background spectra measured with a Cd target on a carbon backing, normalized to the $^{32}$S$(p,t)^{30}$S data. For 10° and 20°, an aluminum plate along the focal plane blocked the channel region greater than ≈2000, where elastically scattered particles reached the focal plane. A few peaks from $^{13}$C$(p,t)^{11}$C are also identified.

The triton peaks were fitted with Gaussian functions to determine the peak centroids. The energy calibration was determined from a combination of known levels of $^{26}$Si (measured with $^{28}$Si$(p,t)^{26}$Si) and of $^{30}$S. The calibration states were the 1796.6-, 2785-, 3334-, and 3756.9-keV levels of $^{26}$Si and the 2210.6-, 3402.6-, and 5136-keV levels of $^{30}$S. The adopted energies are weighted averages of previous work on $^{26}$Si levels [29,30] and on $^{30}$S [23–26]. Polynomial least-squares fits of momentum vs centroid channel were determined for these calibration points at each angle ($0.95 \leqslant \chi^2_\nu \leqslant 2.1$). These fits were used to determine the $^{30}$S excitation energies at each angle, which were then averaged to derive the final excitation energies. In addition to uncertainties derived from the Gaussian fits, a universal uncertainty of 3.0 keV was included due to the uncertainty in the mass of $^{30}$S [15]. The energy resolution was ≈30 keV (FWHM), which is a factor of 3–4 smaller than those of previous $^{32}$S$(p,t)^{30}$S measurements [17,23]. This improvement highlights one advantage of using a magnetic spectrometer over silicon detectors, which were used before.

Six proton unbound states of $^{30}$S with $E_x < 5.5$ MeV were observed, and their energies are listed in Table I. The 4693-keV state is close in energy to the proposed $3^+$ state measured in Ref. [17]. The 4814-keV level, observed here for the first time, is therefore a strong candidate for the astrophysically important $2^+$ state. The other four levels have been previously measured but also have unknown or tentatively assigned spin-parity values (see Table I). However, constraints on the assignments can be obtained from comparisons with the mirror nucleus $^{30}$Si and with guidance from IMME predictions for the $^{30}$S energies. For the latter, our isotensor Coulomb energy term in the IMME [31] was different from that of Ref. [6] by 34%. Energies of $^{30}$S proton unbound states were calculated using an updated compilation of $A = 30$ isobaric levels [32]. The arguments leading to our proposed $J^\pi$ assignments for our states are summarized presently. The adopted mirror assignments between $^{30}$S and $^{30}$Si levels are shown in Fig. 2.

*The 4693-keV level*: Bardayan *et al.* [17] observed a state at 4704(5) keV, to which $J^\pi = 3^+_1$ was assigned based mainly on the IMME prediction of 4733(40) keV of Ref. [6] for its energy. Our measured energy agrees with that of Ref. [17] at the $2\sigma$ level. The energy of this $3^+$ level from our IMME calculations is 4698(30) keV, which agrees with both measured values. We thus also tentatively assign $3^+$ to this state, making it the mirror of the $^{30}$Si $3^+_1$ state at 4831 keV [18].

*The 4814-keV level*: This level has never been observed before. We have tentatively assigned this new state to be the $2^+_3$ level corresponding to the $^{30}$Si $2^+_3$ state at 4810 keV [18]. Our IMME calculations and that of Ref. [6] predict that the next state above the $3^+_1$ level in $^{30}$S should be the $2^+_3$. Although our predicted energy of 4854(30) keV agrees with the 4888(40)-keV prediction of Ref. [6], our measured energy is in disagreement with both predictions at the $1\sigma$ level.

*The 5136-keV level*: In Ref. [25], the spin was constrained to be between 1–4 and $J^\pi = 4^+$ was tentatively assigned. Our IMME calculation predicts the $3^+_2$ level to be at 5148(30) keV, and the next unpaired level in the mirror nucleus $^{30}$Si is the $3^+_2$ level at 5232 keV. Thus, we tentatively assign $J^\pi = 3^+$ to this level, in agreement with Ref. [6].

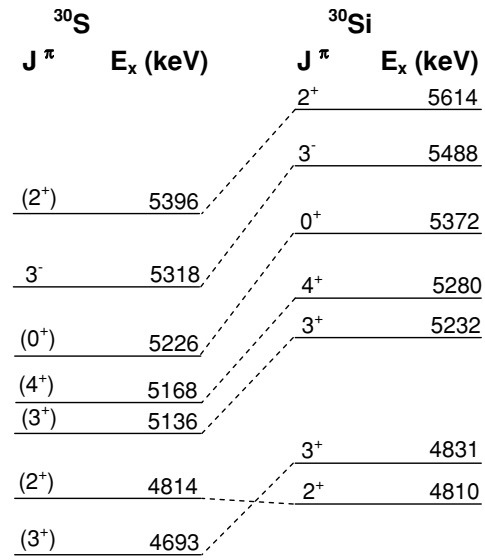


FIG. 2. Level structures of $^{30}$Si [18] and $^{30}$S (present work) above the $^{29}$P + $p$ threshold at 4399 keV and below 5.5 MeV. Dashed lines indicate proposed mirror assignments from the present work (see text).

*The 5226-keV level*: Bardayan *et al.* [17] observed a peak at 5168(6) keV, which was suggested to be an unresolved doublet ($4^+$, $0^+$) based on a distorted-wave Born approximation analysis. We do not observe a peak at this energy, and our 5226(3)-keV level is in agreement with the 5207(22)-keV level seen in the $^{32}$S$(p,t)^{30}$S study of Ref. [23]. In the absence of further experimental information, for our present purposes we assume one level at 5168(6) keV and another at 5217.8(14) keV. The latter is a weighted average of our energy and the energies of Refs. [23,27] (see Table I). We tentatively assign $4^+$ and $0^+$ to the two states, respectively, which is consistent with the order of this pair in $^{30}$Si.

*The 5318-keV level*: Our IMME calculation predicts that the $3^-_1$ level lies near 5.3 MeV. Our 5318-keV level is identified with the 5306(25)- and 5288(10)-keV states observed by Paddock [23] and Yokota *et al.* [26], respectively. The latter determined the spin and parity of this state to be $3^-$.

*The 5396-keV level*: This state is identified with the 5383(8)-keV level seen by Bardayan *et al.* [17], which is matched in Ref. [17] with states near 5.4 MeV seen in Refs. [23,26,27]. Based on spin-parity constraints from Refs. [17,26], and noting that our IMME calculation predicts the $2^+_4$ level to be near 5.4 MeV, we tentatively assign $J^\pi = 2^+$ to this state, in agreement with Ref. [17].

Our results were used to calculate the $^{29}$P$(p,\gamma)^{30}$S reaction rate at temperatures characteristic of explosive nucleosynthesis in novae and x-ray bursts. For the resonant rate, all resonances were treated as isolated and narrow in the temperature range for which the resonance energy falls inside $E_0 \pm 2\Delta$ [34], where $E_0$ and $\Delta$ are the energies of the Gamow peak and window, respectively. Outside this range, the contributions of the resonance wings were calculated numerically.

TABLE II. $^{30}$S level parameters for the $^{29}$P$(p,\gamma)^{30}$S resonant reaction rate (see text for discussion).

| $E_x$[a] (keV) | $E_R$ (keV) | $J^\pi$ | C$^2$S[b] | $l$ | $\Gamma_p$ (eV) | $\Gamma_\gamma$ (eV) | $\omega\gamma$ (eV) |
|---|---|---|---|---|---|---|---|
| 4699(6) | 300(7) | $(3_1^+)$ | 0.04 | 2 | $2.3 \times 10^{-5}$ | $4.9 \times 10^{-3}$ | $4.0 \times 10^{-5}$ |
| 4814(3) | 415(4) | $(2_3^+)$ | 0.11 | 2 | $3.7 \times 10^{-3}$ | $4.8 \times 10^{-3}$ | $2.6 \times 10^{-3}$ |
| 5136(2) | 737(4) | $(3_2^+)$ | 0.02 | 2 | $2.3 \times 10^{-1}$ | $1.1 \times 10^{-2}$ | $1.8 \times 10^{-2}$ |
| 5168(6) | 769(7) | $(4_1^+)$ | $\leqslant$0.01 | 4 | $\leqslant 3.5 \times 10^{-4}$ | $4.8 \times 10^{-3}$ | $7.8 \times 10^{-5}$ |
| 5217.8(14) | 819(3) | $(0_3^+)$ | $\leqslant$0.01 | 0 | $\leqslant 1.8 \times 10^{+1}$ | $6.4 \times 10^{-3}$ | $1.6 \times 10^{-3}$ |
| 5314(7) | 915(8) | $3_1^-$ | 0.36 | 3 | $9.9 \times 10^{-1}$ | $9.7 \times 10^{-3}$ | $1.7 \times 10^{-2}$ |
| 5391(3) | 992(4) | $(2_4^+)$ | 0.05 | 2 | $6.8 \times 10^{+0}$ | $1.8 \times 10^{-2}$ | $2.2 \times 10^{-2}$ |

[a]Weighted averages of the excitation energies listed in Table I.
[b]Spectroscopic factors of mirror states determined from the $^{29}$Si$(d,p)^{30}$Si reaction in the work of Ref. [33].

The proton widths were determined using the expression [34]

$$\Gamma_p = 2\frac{\hbar}{\mu a^2} P_l C^2 S \theta_{\rm sp}^2, \quad (1)$$

where $P_l$ is the barrier penetrability for orbital angular momentum $l$, $a = r_0(A_t^{1/3} + A_p^{1/3})$ is the interaction radius in terms of target $(A_t)$ and projectile $(A_p)$ mass numbers, $\mu$ is the reduced mass, $C$ and $S$ are the isospin Clebsch-Gordan coefficient and spectroscopic factor, respectively, and $\theta_{\rm sp}^2$ is the dimensionless single-particle reduced width.

The penetrabilities were calculated using numerically computed Coulomb wave functions and a radius parameter $r_0 = 1.25$ fm. Spectroscopic factors were determined from neutron spectroscopic factors of the mirror states measured with $^{29}$Si$(d,p)^{30}$Si [33], which is the mirror of the $^{29}$P$(d,n)^{30}$S reaction. The 769- and 819-keV resonances in particular were very weakly populated in the measurement of Ref. [33]. Therefore, $C^2S \leqslant 0.01$ is adopted for these states, based on the sensitivity for the extraction of small spectroscopic factors in that experiment. The dimensionless single-particle reduced widths, $\theta_{\rm sp}^2$, were calculated with the approach of Ref. [35]. The reduced width of the 769-keV resonance, however, could not be determined by this method, which is limited to single-particle states in the $sd$-$fp$ shells. Consequently, $\theta_{\rm sp}^2 \leqslant 1$ is assumed for this state. A standard uncertainty of a factor of 2 in the proton widths $\Gamma_p$ [31] is adopted for all resonances.

To determine the $\gamma$-ray partial widths ($\Gamma_\gamma$), the corresponding widths of the mirror states in $^{30}$Si were calculated from measured half-lives, branching ratios, multipolarities, and mixing ratios [18]. These widths were then scaled to account for the energy difference between each mirror pair, assuming similar decay branches and reduced transition probabilities. An uncertainty of a factor of 2 in $\Gamma_\gamma$ is assumed.

The adopted level parameters are listed in Table II. For the 769- and 819-keV resonances, upper limits were determined for their proton widths. Hence, following the standard procedure of Ref. [36], the adopted resonance strengths ($\omega\gamma$) were calculated with 10% of the upper limits of the proton widths (the lower limits of their strengths are set to be zero).

For the nonresonant contribution, the $^{29}$P$(p,\gamma)^{30}$S direct-capture (DC) reaction rate to all bound states was calculated assuming proton transfer into $2s$ and $1d$ final orbits. For each final state, the $S$ factor was calculated by taking into account the $E1$ and $M1$ nature of the transitions. The transitions were then weighted by the corresponding spectroscopic factors,

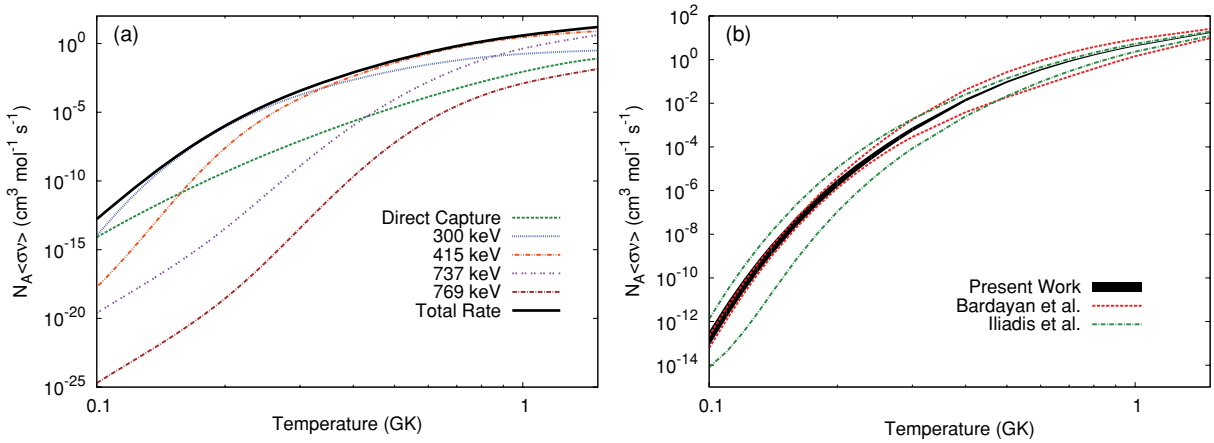


FIG. 3. (Color online) (a) The new thermonuclear $^{29}$P$(p,\gamma)^{30}$S reaction rate as a function of temperature. The 300-keV resonance controls the rate over the temperature range of 0.08 to 0.3 GK. The new 415-keV resonance, in turn, dominates the rate from 0.3 to 1.5 GK. (b) Variation in the present and previously determined reaction rates [6,17] due solely to the uncertainties in the resonance energies.

which were determined from those of the mirror states [33]. Lastly, the DC rate was determined from the sum of the $S$ factors for each transition. The rate was in agreement with that of Bardayan *et al.* [17], with deviations of less than 5%.

The DC rate and the contributions of the four strongest resonances are plotted in Fig. 3, as a function of temperature. The DC rate dominates for $T \lesssim 0.08$ GK. The rate at nova temperatures is dominated by the 300-keV ($3^+$) resonance from 0.08 to 0.3 GK, contributing almost all of the total rate at $T = 0.12$ GK. The new 415-keV ($2^+$) resonance is the main contributor from 0.3 to 1.5 GK, up through the range of interest for explosive nucleosynthesis in x-ray bursts (supplying about 70% at $T = 0.4$ GK). For the higher resonances, at $T = 1.5$ GK, the 737- and 769-keV resonances contribute, respectively, about 30% and less than 1% to the total rate, while the combined contribution of the 819-, 915-, and 992-keV resonances reaches 14%. Our total rate is up to four times larger than the rate of Ref. [17] and up to 20 times larger than that of Ref. [6], due mainly to new measured energies for the two important levels near $E_x = 4.74$–$4.8$ MeV.

In the work of Bardayan *et al.* [17], their calculated rate is compared to that of Ref. [6] by including only the uncertainty in the energy of the 300-keV resonance. For a similar comparison with our new calculated rate, we also first consider uncertainties in $E_r$ only, but expand on the work of Ref. [17] by including those of all the resonances included in the three rates. The resulting upper and lower rate limits are shown in Fig. 3(b). Our rate variation is reduced by up to factors of 7 and 17 relative to those of Refs. [17] and [6], respectively.

To include the resonance strength uncertainties, these were calculated from the uncertainties of the partial widths. New rate limits were determined with the uncertainties of both the resonance energies and the strengths. In the nova temperature regime, the largest variation in our rate is a factor of 17 at $T \approx 0.1$ GK, while in the temperature range of x-ray bursts, the maximum variation is a factor of about 5 at $T \approx 0.9$ GK.

In summary, as a result of this measurement of $^{29}\mathrm{P} + p$ resonance energies in $^{30}$S with improved precision—including the discovery of a new important state—the $^{29}\mathrm{P}(p,\gamma)^{30}\mathrm{S}$ reaction rate is now on firmer empirical ground and its uncertainty range has been significantly reduced. The new calculated rate is now limited by the large uncertainties in the resonance strengths, which are related to spin-parity assignments inferred from mirror state properties. Further indirect studies on $^{30}$S [19–22], and ultimately a direct measurement of the $^{29}\mathrm{P}(p,\gamma)^{30}\mathrm{S}$ reaction with a $^{29}$P radioactive beam, will be invaluable toward reducing the remaining uncertainty in the $^{29}\mathrm{P}(p,\gamma)^{30}\mathrm{S}$ thermonuclear reaction rate and determining its implications for explosive nucleosynthesis.

We thank the WNSL staff for their contributions. This work was supported by the Natural Sciences and Engineering Research Council of Canada; the US Department of Energy under Grants DE-FG02-91ER40609, DE-AC02-06CH11357, and DE-FG02-97ER41020; and the DFG cluster of excellence "Origin and Structure of the Universe."

[1] M. F. Bode and A. Evans, *Classical Novae* (Cambridge University Press, Cambridge, UK, 2008), pp. 128–137.
[2] S. Amari, X. Gao, L. R. Nittler, E. Zinner, J. José, M. Hernanz, and R. S. Lewis, Astrophys. J. **551**, 1065 (2001).
[3] J. José, M. Hernanz, S. Amari, K. Lodders, and E. Zinner, Astrophys. J. **612**, 414 (2004).
[4] L. R. Nittler and P. Hoppe, Astrophys. J. **631**, L89 (2005).
[5] C. Iliadis, A. E. Champagne, J. José, S. Starrfield, and P. Tupper, Astrophys. J. Suppl. Ser. **142**, 105 (2002).
[6] C. Iliadis, J. M. D'Auria, S. Starrfield, W. J. Thompson, and M. Wiescher, Astrophys. J. Suppl. Ser. **134**, 151 (2001).
[7] S. E. Woosley and R. E. Taam, Nature (London) **263**, 101 (1976).
[8] H. Schatz and K. E. Rehm, Nucl. Phys. A **777**, 601 (2006).
[9] J. L. Fisker, H. Schatz, and F.-K. Thielemann, Astrophys. J. Suppl. Ser. **174**, 261 (2008).
[10] H. Schatz *et al.*, Phys. Rep. **294**, 167 (1998).
[11] A. Parikh, J. José, F. Moreno, and C. Iliadis, Astrophys. J. Suppl. Ser. **178**, 110 (2008).
[12] J. L. Fisker, F.-K. Thielemann, and M. Wiescher, Astrophys. J. **608**, L61 (2004).
[13] C. Wrede, J. A. Caggiano, J. A. Clark, C. M. Deibel, A. Parikh, and P. D. Parker, Phys. Rev. C **79**, 045808 (2009).
[14] J. José, F. Moreno, A. Parikh, and C. Iliadis, Astrophys. J. Suppl. Ser. **189**, 204 (2010).
[15] G. Audi, A. H. Wapstra, and C. Thibault, Nucl. Phys. A **729**, 337 (2003).
[16] M. Wiescher and J. Görres, Z. Phys. A **329**, 121 (1988).
[17] D. W. Bardayan *et al.*, Phys. Rev. C **76**, 045803 (2007).
[18] [http://www.nndc.bnl.gov/nudat2/].
[19] D. Galaviz *et al.*, in Proceedings of Science: International Symposium on Nuclear Astrophysics—Nuclei in the Cosmos—IX, Geneva, 2006, PoS(NIC IX) 099.
[20] W. P. Tan *et al.*, Nucl. Phys. A **834**, 679c (2010).
[21] T. Komatsubara (private communication).
[22] J. M. Figueira *et al.*, ATLAS Proposal No. 1242, Argonne National Laboratory, 2008 (unpublished).
[23] R. A. Paddock, Phys. Rev. C **5**, 485 (1972).
[24] J. M. G. Caraça, R. D. Gill, A. J. Cox, and H. J. Rose, Nucl. Phys. A **193**, 1 (1972).
[25] E. Kuhlmann, W. Albrecht, and A. Hoffmann, Nucl. Phys. A **213**, 82 (1973).
[26] H. Yokota, K. Fujioka, K. Ichimaru, Y. Mihara, and R. Chiba, Nucl. Phys. A **383**, 298 (1982).
[27] H. O. U. Fynbo *et al.*, Nucl. Phys. A **677**, 38 (2000).
[28] A. Parikh, Ph.D. thesis, Yale University, 2006.
[29] P. Endt, Nucl. Phys. A **521**, 1 (1990).
[30] D. Seweryniak *et al.*, Phys. Rev. C **75**, 062801(R) (2007).
[31] C. Iliadis, P. M. Endt, N. Prantzos, and W. J. Thompson, Astrophys. J. **524**, 434 (1999).
[32] M. S. Basunia, Nucl. Data Sheets (to be published).
[33] H. Mackh, H. Oeschler, G. J. Wagner, D. Dehnhard, and H. Ohnuma, Nucl. Phys. A **202**, 497 (1973).
[34] C. Iliadis, *Nuclear Physics of Stars* (Wiley-VCH, Weinheim, 2007).
[35] C. Iliadis, Nucl. Phys. A **618**, 166 (1997).
[36] C. Angulo *et al.*, Nucl. Phys. A **656**, 3 (1999).